



# Outstanding role of the magnetic entropy in arrested austenite in an ordered $\text{Ni}_{45}\text{Mn}_{36.7}\text{In}_{13.3}\text{Co}_5$ metamagnetic shape memory alloy

J.I. Pérez-Landazábal<sup>a,b,\*</sup>, V. Recarte<sup>a,b</sup>, V. Sánchez-Alarcos<sup>a,b</sup>, M. Jiménez Ruiz<sup>c</sup>, E. Cesari<sup>d</sup>

<sup>a</sup> Departamento de Ciencias, Universidad Pública de Navarra, Campus de Arrosadía, 31006 Pamplona, Spain

<sup>b</sup> Institute for Advanced Materials (INAMAT), Universidad Pública de Navarra, Campus de Arrosadía, 31006 Pamplona, Spain

<sup>c</sup> Institut Laue Langevin, 71, Avenue des Martyrs, CS 20156, 38042 Grenoble Cedex 9, France

<sup>d</sup> Departament de Física, Universitat de les Illes Balears, Ctra. de Valldemossa, km 7.5, E-07122 Palma de Mallorca, Spain

## ARTICLE INFO

### Article history:

Received 18 January 2019

Received in revised form 11 April 2019

Accepted 29 April 2019

Available online 2 May 2019

### Keywords:

Ferromagnetic shape memory alloys

Martensitic phase transformation

Thermodynamics

Magnetic entropy

## ABSTRACT

The relevance of the entropy and in particular the outstanding role of the magnetic contribution is analyzed in a non-equilibrium arrested austenite phase in a  $\text{Ni}_{45}\text{Mn}_{36.7}\text{In}_{13.3}\text{Co}_5$  metamagnetic shape memory alloy. The Debye and Bragg-Williams approximations have been used to analyze and quantify the vibrational and magnetic contributions respectively, to the total entropy change linked to the martensitic transformation. The sign on the entropy change associated to the forward austenite to martensite transformation is different depending on whether it occurs at low or at high temperature as a consequence of the different vibrational and magnetic contributions.

© 2019 Acta Materialia Inc. Published by Elsevier Ltd. All rights reserved.

Producing cold is much more difficult than producing heat but is critical for many applications of everyday life like food preservation, cooling device or air conditioning. Refrigeration means reaching temperatures below that of the surrounding environment and involves entropy transferences. From a technological point of view it also involves isolation, heat release, energy consumption, noise and so on, all clearly noticeable in typical refrigeration devices. The search for an alternate technology to replace the conventional devices based on gas compression-expansion sequences is one of the topics of increasing interest in this field [1,2]. Cooling and heating a system in non-adiabatic conditions is a phenomenon directly related to total entropy changes. This global entropy change results from the contribution of the entropy change of different subsystems (vibrational, elastic, configurational, magnetic, electronic etc.). As a consequence, the entropy can be changed by variation of external parameters like magnetic field, applied stress, pressure, electric field and other thermodynamic parameters. In particular, the magnetic contribution to the entropy and its change are closely related to the Magnetocaloric Effect (MCE). For example, the temperature can be modified by magnetization of the system that raise their temperatures when adiabatically magnetized, and drop their temperature when adiabatically demagnetized. In order to understand the MCE and its correlation to the magnetic entropy, Landau theories have been used [3] to analyze the phase transition itself and the

processes of approach to equilibrium [3–6]. In this way, magnetic materials exhibiting large MCE are promising candidates [7,8].

The active system in magnetic refrigeration is a ferromagnetic material which usually undergoes first and/or second order phase transitions. Metamagnetic Shape Memory Alloys (MSMA) are examples of such a kind of materials. Some MSMA provides a peculiar behavior on cooling under high magnetic fields. These alloys exhibit a thermoelastic Martensitic Transformation (MT) from a ferromagnetic high temperature phase (austenite) to a weakly magnetic low temperature phase (martensite) [9–15]. The magnetostructural MT is mainly driven by the coupled magnetism and lattice characteristics of both phases [4–6,16]. In particular, the entropy change linked to the MT is usually considered as the sum of vibrational, and magnetic terms ( $\Delta S = \Delta S_{\text{vib}} + \Delta S_{\text{mag}}$ ) although an elastic contribution has also be taken into account [17]. The electronic contribution is expected to be very small [18–20].

The low energy transverse acoustic  $\text{TA}_2[110]$  phonon branch of the cubic phase, shows an anomalous decrease of its phonon frequencies on cooling to the MT temperature [21–25] and induces an instability of the cubic phase towards martensitic structures. Since the martensite phonon spectrum shows no soft modes [26], the vibrational entropy always decreases in the austenite to martensite forward MT and therefore  $\Delta S_{\text{vib}} < 0$ . On the other hand, the sign of  $\Delta S_{\text{mag}}$  is positive in metamagnetic alloys where the martensitic phase is paramagnetic-like and the austenite ferromagnetic ( $\Delta M < 0$ ) [27,28]. Classic thermodynamics establishes that  $\Delta S$  must be negative in order the MT to takes place. Nevertheless, the application of a magnetic field may lead to an increase of the positive magnetic entropy change associated with the

\* Corresponding author at: Departamento de Ciencias, Universidad Pública de Navarra, Campus de Arrosadía, 31006 Pamplona, Spain.

E-mail address: [ipzlanda@unavarra.es](mailto:ipzlanda@unavarra.es) (J.I. Pérez-Landazábal).

forward MT that can counterbalance the negative vibrational term, thus resulting in the magnetic arrest of the MT [6,29–34]. The microstructural origin of the arrest has been recently studied [35].

In this paper, the magnetic field induced entropy is analyzed in a non-equilibrium arrested austenite achieved in a metamagnetic shape memory alloy. The possibility to arrest the austenite at low temperatures allows a peculiar and interesting scenario (otherwise impossible) to demonstrate the key role of the magnetic contribution. Using Debye and Bragg-Williams approximations the vibrational and magnetic contributions has been quantified. As a consequence of their counterbalance contribution, the sign on the entropy change associated to the forward austenite to martensite transformation is different depending on whether it occurs at low or at high temperature.

A  $\text{Ni}_{45}\text{Mn}_{36.7}\text{In}_{13.3}\text{Co}_5$  alloy was produced by arc-melting followed by several consecutive re-melting in order to homogenize the ingot. After 24 h homogenization at 1170 K under vacuum, samples were annealed at 1070 K for 1800 s and slowly cooled in air to obtain an ordered alloy. In this conditions, the MT at  $T_m = 258$  K (DSC Peak maximum on cooling) occurs between a ferromagnetic austenite and a martensitic phase formed by magnetic interacting clusters inside a paramagnetic matrix [36]. The Curie temperature of the alloy is  $T_c = 386$  K. For the current purposes, the alloy behaves as a paramagnetic martensite. Previous works [37] have shown that, around 70% of austenite is retained or arrested at 10 K without magnetic field after cooling the alloy under a strong enough magnetic field (above 5.5 T). On heating, an “anomalous” forward austenite to martensite MT first occurs (FMTH) and then a complete standard reverse MT at higher temperatures follows. On the other side, the standard forward MT occurs on cooling (FMTC) under a Zero Field Cooling (ZFC) process. Therefore, the same forward austenite to martensite transformation can be produced by heating and by cooling. Fig. 1 summarizes the demagnetization induced entropy changes linked to both forward martensitic transformations as a function of temperature and magnetic field (see ref. 37 for experimental details). The field reduction or demagnetization process produces a positive  $\Delta S$  entropy change in the FMTH while shows negative values in the FMTC.

Nevertheless, the field reduction in both situations induces the same transformation i.e. from high magnetic moment austenite to low magnetic moment martensite. This leads to the peculiar situation where the sign on the entropy change associated to the austenite to martensite transformation is different depending on whether it occurs at low or at high temperatures. The relevance of the entropy contributions and in particular the outstanding role of the magnetic entropy must be understood to analyze in detail this effect. To avoid confusion, the entropy change  $\Delta S$  is always assessed from martensite to austenite:  $\Delta S = \Delta S^{\text{mar}} - \Delta S^{\text{aus}}$ .

The Debye temperature is not a constant but usually its value in the so-called low-temperature limit is used. So, only the low-energetic long-wavelength phonons of the lattice vibrations are excited. In this way, the values of the elastic constants can be used to determine the Debye temperature ( $\theta_D$ ) of the austenite phase [38]. The vibrational behavior of the austenite in a ordered  $\text{Ni}_{45}\text{Mn}_{36.7}\text{In}_{13.3}\text{Co}_5$  single crystal has been analyzed through the phonon branches measured by Inelastic Neutron Scattering and shown in Fig. 2 (upper inset). A rectangular parallelepiped of  $9 \times 4 \times 4$  mm<sup>3</sup> oriented with the edges parallel to the (100) directions were prepared for the inelastic neutron experiments. Neutron scattering experiments were carried out on the thermal neutron triple axis spectrometer IN3 at the Institute Laue-Langevin. The optimal conditions for accessing the TA<sub>2</sub>-phonon with a good energy resolution were found to be those employing the PG (002) monochromator and PG (002) analyzer, and a constant final wave vector  $k_f = 2.662 \text{ \AA}^{-1}$ .

Transversal and longitudinal phonon dispersion curves measured along the high symmetry directions  $[\xi 0 0]$  and  $[\xi \xi 0]$  at 300 K are shown in Fig. 2 (upper inset). The TA [100] and LA [110] curves do not show any anomaly. In contrast, the transversal TA<sub>2</sub> mode energies slightly higher and the dip (appears for wave numbers  $\xi = 0.3$ – $0.4$  along  $[\xi \xi 0]$ ) less pronounced than those reported in other alloy systems [39–43]. The elastic constants determined from the initial slope of the curves are  $C_{11} = 160 \pm 30$  GPa,  $C_{12} = 130 \pm 30$  GPa,  $C_{44} = 70 \pm 7$  GPa and  $C' = 13 \pm 3$  GPa. On the other hand, the Debye temperature of the martensite can be measured in a more direct way through the

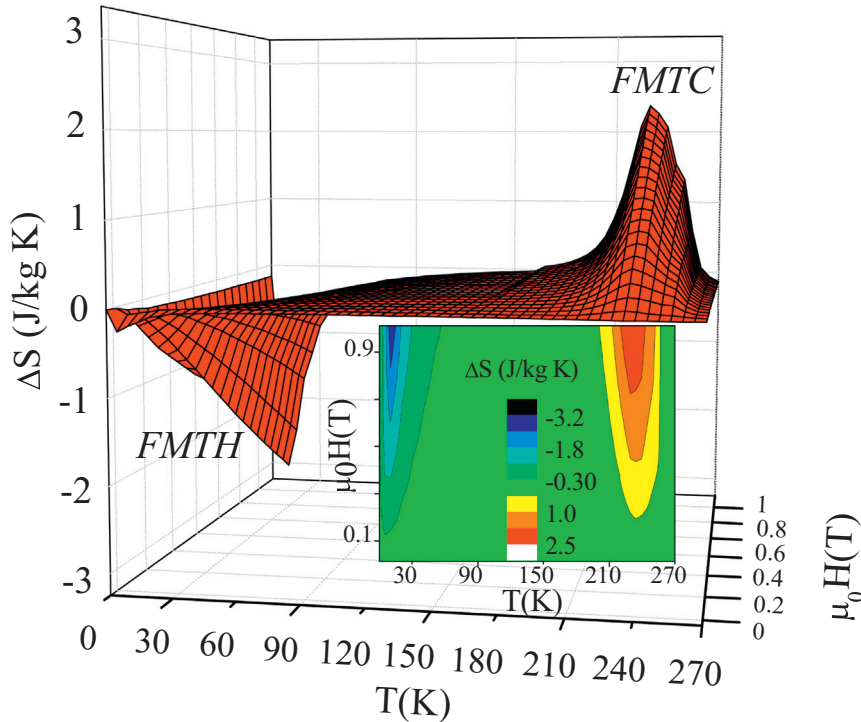
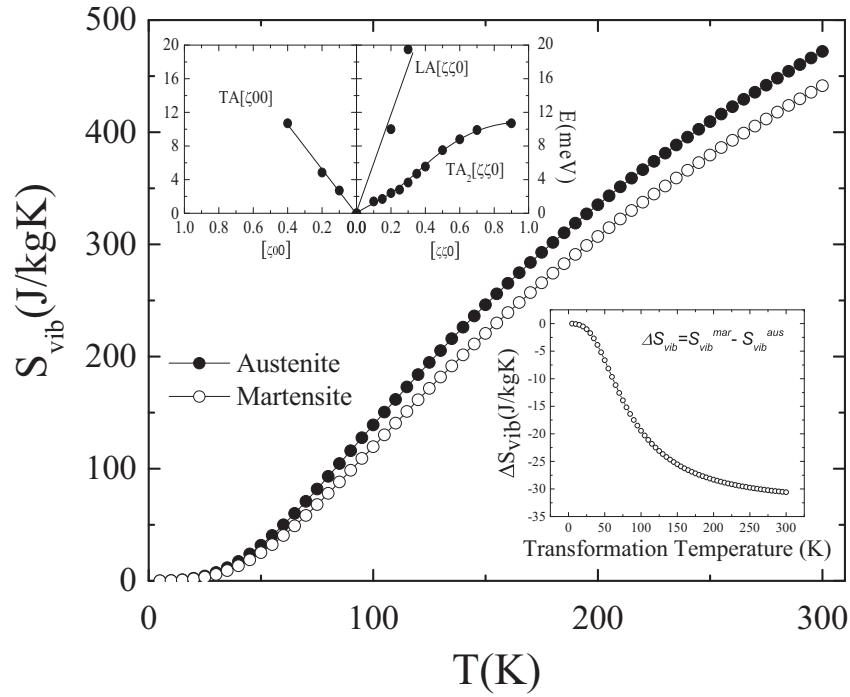


Fig. 1. Magnetic field induced entropy change  $\Delta S(T, H) = S(T, H) - S(T, 0)$  (field removing) linked to both FMTH and FMTC as a function of temperature and magnetic field. The projection shows the qualitative intensity of the entropy changes.



**Fig. 2.** Debye model for the vibrational entropy for austenite and martensite as a function of temperature. The lower inset shows the entropy change  $\Delta S_{vib}$  from austenite to martensite as a function of the MT temperature. The upper inset shows the TA along the  $[100]$  and L and  $TA_2$  phonon branches along the  $[110]$  direction of the austenite at room temperature.

heat capacity measured at low temperatures [37]. The obtained values ( $\theta_D = 310 \pm 25$  K for austenite and  $\theta_D = 340 \pm 4$  K for martensite) allows the determination of the vibrational entropy ( $S_{vib}$ ) of both phases [44], according to the expression:

$$S_{vib}(T) = \frac{12Nk_B}{\omega_D^3} \int_0^{\omega_D} \frac{(\hbar\omega^3/k_B T)}{(\exp(\hbar\omega/k_B T) - 1)} d\omega - 3Nk_B \ln[1 - \exp(\hbar\omega_D/k_B T)] \quad (1)$$

where  $\hbar\omega_D = k_B\theta_D$ .

The temperature dependence of the vibrational entropy is different in austenite and martensite as shown in Fig. 2 but at low temperatures in both cases goes to zero. So, depending on the MT temperature the vibrational entropy change is different. The lower inset in Fig. 2 shows the calculated entropy change  $\Delta S_{vib}$  from austenite to martensite as a function of the MT temperature. As expected the change is always negative approaching to zero in the low temperature limit.

On the other side, the magnetic contribution to the entropy can be analyzed within the Bragg-Williams approximation [45]. Assuming a model of Spin Up/Spin Down configurations, the magnetic entropy per

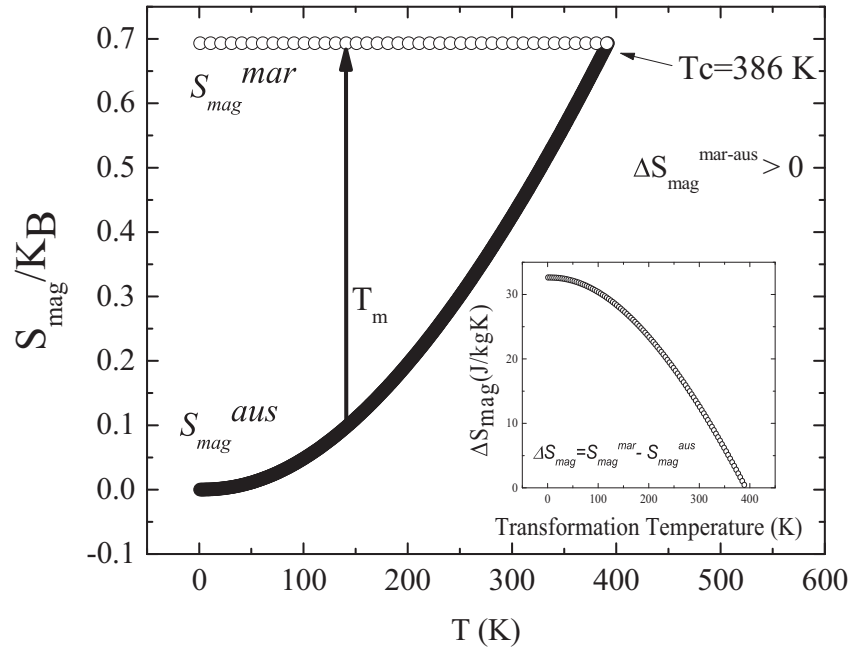


**Fig. 3.** Temperature dependence of the magnetic entropy per atom for both martensite (paramagnetic) and austenite (ferromagnetic). The entropy change (indicated by an arrow) depends on the transformation temperature ( $T_m$ ). The inset shows the calculated entropy change  $\Delta S_{mag}$  from austenite to martensite as a function of the MT temperature.

atom ( $S_{mag}/N$ ) associated with a given normalized magnetization  $m$  is just the logarithm of the total number of possible configurations:

$$\frac{S_{mag}}{N} = k_B \left[ \ln(2) - \frac{1}{2}(1+m)\ln(1+m) - \frac{1}{2}(1-m)\ln(1-m) \right] \quad (2)$$

Fig. 3 shows the temperature dependence of the magnetic entropy for both martensite and austenite. The martensitic phase being paramagnetic has a constant value of the magnetic entropy. On the other side, the entropy of the austenite depends on the magnetization value. Again the change in magnetic contribution to entropy change depends on the MT temperature as shown in the inset in Fig. 3. In this case, the calculated magnetic contribution is always positive and the lower is the temperature the higher the contribution. The arrow in Fig. 3 indicated the entropy change if the transformation takes place at an arbitrary  $T_m$ .

The total entropy change  $\Delta S = \Delta S_{vib} + \Delta S_{mag}$  is shown in Fig. 4 as the addition of both magnetic and vibrational contributions. First of all, the picture shows how the total arrest of the transformation occurs at around 150 K. Assuming a non-temperature dependence of the entropy and enthalpy around the MT, the driving force for the martensitic transformation can be written as  $\Delta G \approx -\Delta S \Delta T$ . So, if the entropy change runs out, the transformation cannot anymore proceed. But the important point to remark is that at high temperatures the austenite to martensite transformation shows a negative entropy change indicating that  $S^{mar} < S^{aus}$ . On the contrary, at low temperatures, the total entropy change is positive and  $S^{mar} > S^{aus}$ . This means that at low temperatures a magnetic field reduction induces a transformation from ferromagnetic austenite to paramagnetic martensite and the measured entropy change is positive. On the other side, at high temperature a magnetic field reduction induces the same transformation but now the entropy change is negative. This analysis explains the different sign found in the entropy changes for the same forward martensite to austenite transformation and highlights the relevance of the entropy contributions and in particular the outstanding role of the magnetic entropy. The proposed analysis about the role of magnetic contribution could be extrapolated to other metamagnetic systems where the counterbalanced magnetic and vibrational contributions control first order magneto-structural transitions.

In summary, the Debye and Bragg-Williams approximations allow to understand and quantify the vibrational and magnetic contributions to the total entropy linked to the martensitic transformation. The analysis has been performed in a peculiar out of equilibrium situation (arrested

austenite) in a metamagnetic shape memory alloy. The retention of ferromagnetic austenite at low temperatures and its transformation to martensite on heating allows the study of a thermodynamic state where the predominance of the magnetic contribution in the entropy plays a crucial role; the sign on the entropy change (and consequently the temperature change) associated to the austenite to martensite transformation is different depending on whether it occurs at low or at high temperature.

## Acknowledgements

This work has been carried out with the financial support of the Spanish “Ministerio de Economía y Competitividad” (AEI/FEDER,UE) (Project numbers MAT2015-65165-C2-R and MAT2014-56116-C4-1-R). The Institute Laue-Langevin is acknowledged for the allocated neutron beamtime (Test 1897).

## References

- [1] X. Moya, S. Kar-Narayan, M.D. Nat. Mater. 13 (2014) 439.
- [2] S. Fähler, V.K. Pecharsky, MRS Bull. 43 (2018) 264.
- [3] V.A. L'vov, A. Kosogor, J.M. Barandiaran, V.A. Chernenko, J. Appl. Phys. 119 (2016), 013902.
- [4] V.A. L'vov, E. Cesari, V. Recarte, J.I. Pérez-Landazábal, Acta Mater. 61 (2013) 1764.
- [5] V.A. L'vov, E. Cesari, J.I. Pérez-Landazábal, V. Recarte and J. Torrens-Serra, J. Phys. D. Appl. Phys. 49 (2016), 095002.
- [6] A.G. Danilevich, V.A. L'vov, J. Phys. D. Appl. Phys. 49 (2016), 105001.
- [7] A.M. Tishin, Y.I. Spichkin, The Magnetocaloric Effect and its Applications, Series in Condensed Matter Physics, Institute of Physics, Bristol, UK, 2003.
- [8] V.K. Pecharsky, K.A. Gschneidner, Phys. Rev. Lett. 78 (1997) 4494.
- [9] Y. Sutou, Y. Imano, N. Koeda, T. Omori, R. Kainuma, K. Ishida, K. Oikawa, Appl. Phys. Lett. 85 (2004) 4358.
- [10] T. Krenke, M. Acet, E.F. Wassermann, X. Moya, L.I. Mañosa, A. Planes, Phys. Rev. B 72 (2005), 014412.
- [11] T. Krenke, M. Acet, E.F. Wassermann, X. Moya L.I. Mañosa, A. Planes, Phys. Rev. B 73 (2006), 174413.
- [12] Y. Koshida, S. Pandey, A. Quetz, A. Aryal, I. Dubenko, J. Cwik, E. Dilmieva, A. Granovsky, E. Lähderanta, S. Stadler and N. Ali, J. of Mag and Magnet. Mater 459 (2018) 98.
- [13] N.U. Hassan, I.A. Shah, A. Rauf, J. Liu, Y. Gong, F. Xu, Mat. Res. Express 5 (2018), 026108.
- [14] F. Chen, Y.X. Tong, L. Li, J.L. Sánchez Llamazares, C.F. Sánchez-Valdés, P. Müllner, J. Alloys Compd. 727 (2017) 603.
- [15] R. Kainuma, Y. Imano, W. Ito, Y. Sutou, H. Morito, S. Okamoto, O. Kitakami, K. Oikawa, A. Fujita, T. Kanomata, K. Ishida, Nature 439 (2006) 957.
- [16] J.M. Barandiaran, V.A. Chernenko, E. Cesari, D. Salas, P. Lazpita, J. Gutierrez, I. Orue, Appl. Phys. Lett. 102 (2013), 071904.
- [17] A. Kosogor, J.M. Barandiaran, V.A. L'vov, J. Rodríguez Fernandez and V.A. Chernenko, J. Appl. Phys. 121 (2017) 183901.
- [18] V.V. Khovaylo, K. Oikawa, T. Abe, T. Tagaki, J. Appl. Phys. 93 (2003) 8483.
- [19] V. Recarte, M. Zbiri, M. Jiménez-Ruiz, V. Sánchez-Alarcos, J.I. Pérez-Landazábal, J. Phys. Condens. Matter 28 (2016), 205402.
- [20] T. Kihara, X. Xu, W. Ito, R. Kainuma, M. Tokunaga, Phys. Rev. B 90 (2014), 214409.
- [21] A. Planes, L.I. Mañosa, Solid State Phys. 55 (2001) 159.
- [22] A. Zheludev, S.M. Shapiro, P. Wochner, A. Schwartz, M. Wall, L.E. Tanner, Phys. Rev. B 51 (1995), 11310.
- [23] X. Moya, L.I. Mañosa, A. Planes, T. Krenke, M. Acet, V.O. Garlea, T.A. Lograsso, D.L. Schlager, J.L. Zaretsky, Phys. Rev. B 73 (2006), 64303.
- [24] T. Mehaddene, J. Neuhaus, W. Petry, K. Hradil, P. Bourges, A. Hiess, Phys. Rev. B 78 (2008), 2104110.
- [25] J.I. Pérez-Landazábal, V. Recarte, V. Sánchez-Alarcos, J.A. Rodríguez-Velamazán, M. Jiménez-Ruiz, P. Link, E. Cesari, Y.I. Chumlyakov, Phys. Rev. B 80 (2009), 144301.
- [26] M.A. Uijttewaal, T. Hickel, J. Neugebauer, M.E. Gruner, P. Entel, Phys. Rev. Lett. 102 (2009), 035702.
- [27] S. Kustov, M.L. Corró, J. Pons and E. Cesari, E. Appl. Phys. Lett. 94 (2009), 191901.
- [28] V. Recarte, J.I. Pérez-Landazábal, V. Sánchez-Alarcos, V. Zablotskii, E. Cesari, S. Kustov, Acta Mater. 60 (2012) 3168.
- [29] V.K. Sharma, M.K. Chattopadhyay, S.B. Boy, Phys. Rev. B 76 (2007), 140401.
- [30] W. Ito, K. Ito, R.Y. Umetsu, R. Kainuma, K. Koyama, K. Watanabe, A. Fujita, K. Oikawa, K. Ishida, Appl. Phys. Lett. 92 (2008), 021908.
- [31] R.Y. Umetsu, W. Ito, K. Ito, K. Koyama, A. Fujita, K. Oikawa, T. Kanomata, R. Kainuma, K. Ishida, Scr. Mater. 60 (2009) 25.
- [32] X. Xu, W. Ito, M. Tokunaga, R.Y. Umetsu, R. Kainuma, K. Ishida, Mater. Trans. 51 (2010) 1357.
- [33] J.I. Pérez-Landazábal, V. Recarte, V. Sánchez-Alarcos, C. Gómez-Polo, S. Kustov, E. Cesari, J. Appl. Phys. 109 (2011), 093515.
- [34] X. Xu, W. Ito, M. Tokunaga, R.Y. Umetsu, R. Kainuma, K. Ishida Mater. Trans 51 (2010) 469.
- [35] N.M. Bruno, D. Salas, S. Wang, V. Igor, R. Roshchin, R. Santamarta, T. Arroyave, Y.I. Duong, I. Karaman Chumlyakov, Acta Mater. 142 (2018) 95.

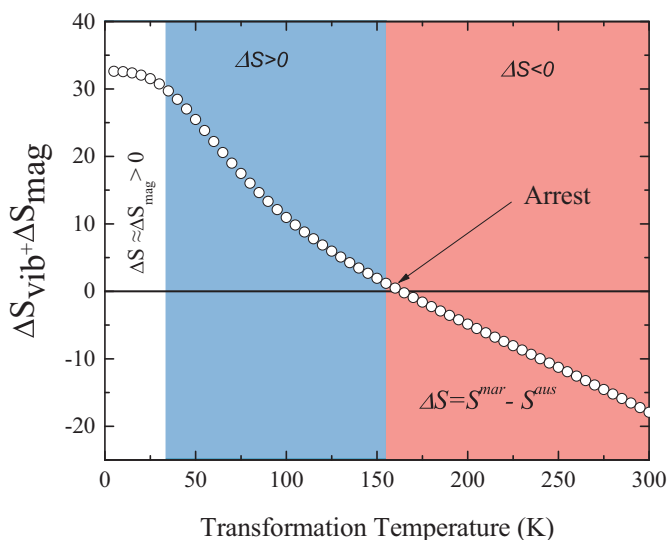


Fig. 4. Temperature dependence of the total entropy change from austenite to martensite as a function of the MT temperature.

- [36] J.I. Pérez-Landazábal, V. Recarte, V. Sánchez-Alarcos, C. Gómez-Polo, E. Cesari, Appl. Phys. Lett. 102 (2013), 101908.
- [37] J.I. Pérez-Landazábal, V. Recarte, V. Sánchez-Alarcos, J.J. Beato-López, J.A. Rodríguez-Velamazan, J. Sánchez-Marcos, C. Gómez-Polo, E. Cesari, Sci. Rep. 7 (2017), 13328.
- [38] H. Siethoff, Intermetallics 5 (1997) 635.
- [39] A. Zheludev, S.M. Shapiro, P. Wochner, A. Schwartz, M. Wall, L.E. Tanner, Phys. Rev. B 51 (1995), 11310.
- [40] A. Zheludev, S.M. Shapiro, P. Wochner, L.E. Tanner, Phys. Rev. B 54 (1996) 15045.
- [41] L. Mañosa, A. Gonzalez-Comas, E. Obradó, A. Planes, V.A. Chernenko, V.V. Kokorin, E. Cesari, Phys. Rev. B 55 (1997), 11068.
- [42] U. Stuhr, P. Vorderwisch, V.V. Kokorin, P.A. Lindgard, Phys. Rev. B 56 (1997), 14360.
- [43] L. Mañosa, A. Planes, J. Zarestky, T. Lograsso, D.L. Schlagel, C. Stassis, Phys. Rev. B 64 (2001), 024305.
- [44] G. Grimvall, Thermophysical Properties of Materials, Elsevier, Amsterdam, 1999.
- [45] P.M. Chaikina, L.C. Lubensky, Principles of Condensed Matter Physics, Cambridge University Press, Cambridge, 1995.